Quercetin, a functional compound of onion peel, remodels white adipocytes to brown-like adipocytes

Sang Gil Lee[a], John S. Parks[b], and Hye Won Kang[a,*]

[a] Food and Nutritional Sciences, Department of Family and Consumer Sciences, North Carolina Agricultural and Technical State University, Greensboro, North Carolina, 27411

[b] Department of Internal Medicine-Section on Molecular Medicine, Wake Forest School of Medicine, Winston-Salem, North Carolina, 27101

* Corresponding author: Hye Won Kang
1601 E. Market Street, Department of Family and Consumer Sciences, North Carolina Agricultural and Technical State University, Greensboro, North Carolina, 27411, Phone: 1-336-285-4858, FAX: 1-336-334-7239, Email: hkang@ncat.edu

Running title: Browning of white adipocytes by quercetin rich-onion peel

This work was supported by the United States Department of Agriculture (NC.X-288-5-15-170-1).

Keywords: browning effect, onion peel, quercetin, uncoupling protein 1, retroperitoneal fat, AMP-activated protein kinase

Abstract

Adipocyte browning is a promising strategy for obesity prevention. Using onion peel-derived extracts and their bioactive compounds, we demonstrate that the onion peel, a by-product of the onion, can change the characteristics of white adipocytes to those of brown-like adipocytes in the white adipose tissue of mice and in 3T3-L1 cells. Expression of the following brown adipose tissue-specific genes was increased in the retroperitoneal and subcutaneous adipose tissues of 0.5% onion peel extract-fed mice: PR domain-containing 16, peroxisome proliferator-activated receptor gamma coactivator 1α, uncoupling protein 1, and cell death-inducing DFFA-like effector. In 3T3-L1 adipocytes, onion peel extract induced the expression of brown adipose tissue-specific genes and increased carnitine palmitoyltransferase 1α. This effect was supported by decreased lipid levels and multiple small-sized lipid droplets. The ethyl acetate fraction of the onion peel extract that contained highest portion of hydrophobic molecules showed the same browning effect in 3T3-L1 adipocytes. A high performance liquid chromatography analysis further identified quercetin as a functional compound in the browning effect by onion peel. The quercetin-associated browning effect was mediated in part by activation of AMP-activated protein kinase. In summary, our study is the first to demonstrate the browning effects of onion peel and quercetin using both animal and cell models. This result indicates that onion peel has the potential to prevent obesity by remodeling the characteristics of white adipocytes to those of brown-like adipocytes.

1. Introduction

Obesity, indicated by excess fat accumulation in white adipose tissue (WAT), mainly develops when energy expenditure is less than energy intake [1]. Long-term excess fat deposition in the body is associated with chronic diseases, including cardiovascular disease, diabetes, and insulin resistance [2]. Increased energy expenditure is crucial to successfully reducing body fat (i.e., weight loss) in obese individuals [1]. Physical activities, including exercise, are interventions that increase energy expenditure and are commonly combined with dietary modifications [1]. Because energy expenditure through exercise require steady and long-term efforts to reduce body fat, the long-term maintenance of a healthy body is difficult for obese people.

The discovery of brown adipose tissue (BAT) in human adults and children has provided a new approach toward increasing energy expenditure [3, 4]. In contrast to WAT, which stores extra energy as fat, BAT expends energy, i.e., stored fat, by generating heat through non-shivering thermogenesis [5]. Uncoupling protein 1 (UCP1), a BAT-specific thermogenin, promotes this heat generation by leaking protons into the mitochondrial matrix to uncouple oxidative phosphorylation from ATP synthesis [6]. Notably, the induction of UCP1 expression contributes to fat reduction in obese people [7]. Thus, UCP1 expression has been indicated as a therapeutic target to increase energy expenditure. In response to physiological stimuli, such as exposure to cold temperatures, some adipocytes in WAT are differentiated into brown like-adipocytes, known as beige or brite adipocytes, that acquire UCP1 expression [8]. This process requires the same major transcriptional factors and indicators as those used to develop brown adipocytes, and they include PR domain-containing 16 (PRDM16), peroxisome proliferator-activated receptor gamma coactivator 1α (PGC1α), and cell death-inducing DFFA-like effector (CIDEA) [9]. Therefore, the browned

white adipocytes may be able to prevent obesity through a UCP1-induced thermogenic effect by burning fat that is directly stored in WAT [5]. Recent studies have indicated that phytochemicals, including curcumin, berberine, capsaicin, monoterpene, and resveratrol, enhance adipocyte browning in WAT [10-14]. However, phytochemicals with browning effects have not been heavily investigated.

Onion peel is a by-product of the onion. It contains high levels of quercetin derivatives, a flavonoid subgroup known as the flavonols, compared with those of the onion and other vegetables and fruits [15]. Quercetin has shown various biological functions, including anti-oxidant, anti-inflammatory, and anti-obesity effects [15-18]. Onion peel extract has been reported to inhibit lipogenesis and adipogenesis and increases fatty acid oxidation [15, 17]. However, the effects of onion peel extract on adipocyte browning in WAT remain unexplored. The aims of this study were to examine the browning effects of onion peel extract in WAT using high fat diet-induced obese C57BL/6 mice and to investigate the onion peel extract-derived compounds for adipocyte browning and its underlying mechanism using 3T3-L1 cells.

2. Materials and methods

2.1. Onion peel extraction

Onion peels were kindly provided by Boardman Foods Inc. (Boardman, Oregon, USA). Fresh onion peels were washed and air-dried overnight. One hundred grams of dried onion peel were pulverized using a homogenizer (Kinematica, New York, USA) for 3 min with 1 L of 60% aqueous ethanol as the extracting solvent. To increase the extraction rate, the homogenized sample was further extracted in an ultrasonic bath for 20 min at room temperature. The extract was filtered through Whatman No. 2 filter paper (Whatman International Limited, Kent, England) using a chilled Büchner funnel. The filtration residues

were extracted once more using the procedure described above. The solvent of the filtrate was evaporated using a rotary evaporator (Buchi RE120 Rotovapo, Flawil, Switzerland) in a water bath at 45 °C until the solvent was completely removed. The onion peel extract (OPE) was scraped from the evaporator flask and stored at -80 °C until use.

2.2. Fractionation of OPE by liquid-liquid extraction

OPE was fractionated into the ethyl acetate fraction (OPEF) and water fraction (OPWF) using the liquid-liquid extraction method. Briefly, 20 g of OPE was dissolved in 200 mL of deionized water (DW) and transferred to a separatory funnel. After adding an equal volume of ethyl acetate to the separatory funnel, the mixture was vigorously shaken and maintained overnight at room temperature. The mixture was divided into the ethyl acetate layer (OPEF) and water layer (OPWF) according to the immiscibility of solvents. All OPE fractions were separately collected and evaporated using a rotary evaporator until they were completely dried. The fractions were stored at -80 °C until use.

2.3. Identification and quantification of the main compounds in OPE, OPEF, and OPWF by reversed-phase high-performance liquid chromatography *(HPLC)*

HPLC was performed to identify and quantitate the major compounds in OPE, OPEF, and OPWF using a Waters HPLC system (Waters, Milford, MA, USA) equipped with a 1525 binary pump and 2748 dual wavelength absorbance detector (DAD). Separations were performed on a C_{18} reversed-phase symmetry analytical column (5 μm x 300 mm x 4.6 mm; Waters, Milford, MA) using a gradient of mobile phases at a flow rate of 1.0 mL/min. The gradient elution was performed by changing the ratio of solvent A (HPLC-grade water with 0.5% H_3PO_4) to solvent B (methanol with 0.5% H_3PO_4) as follows: 95% A and 5% B, 0-10 min; 85% A and 15% B, 10-15 min; 70% A and 30% B, 15-20 min; 65% A and 35% B, 20-

25 min; 30% A and 70% B, 25-28 min; and 95% A and 5% B, 28-30 min. The injection volume for each sample was 10 µL. The detection was performed at 360 nm. Quercetin and isoquercetin in OPE, OPEF, and OPWF were quantitated by comparing their retention times to those of pure quercetin and isoquercetin standards (Sigma-Aldrich, St. Louis, MO, USA). All organic solvents used in the analysis were HPLC grade (Thermo Fisher Scientific, Waltham, MA, USA).

2.4. Animal study

Fifteen 4-week-old male C57BL/6 mice were purchased from the Jackson Laboratory (Bar Harbor, ME, USA). The mice were randomly assigned to two dietary groups as follows: one was fed a high-fat diet (HFD, 60% Kcal from fat, n = 9) and the other was fed HFD supplemented with 0.5% OPE (w/w, HFD-OPE, n = 6). The diets were established in the Comparative Medicine Diet Laboratory at Wake Forest School of Medicine (Winston-Salem, NC, USA) (Supplementary Table 1). The mice were housed in a room maintained at 25 °C with a 12-h light-dark cycle and provided with free access to food and water for 8 weeks. Their body weights and dietary consumption were recorded weekly. At the end of the experimental feeding, mice were fasted for 16 h and anesthetized with isoflurane using a Somnosuit-small animal anesthesia system (Kent Scientific Cooperation, St. Torrington, CT, USA). Blood was drawn by cardiac puncture under anesthesia using a syringe that contained ethylenediaminetetra acetic acid. Plasma was separated from the whole blood by centrifugation at 12,000 x g for 10 min at 4 °C. The mice were euthanized by cervical dislocation. The epididymal WAT (EWAT), retroperitoneal WAT (RWAT) and subcutaneous WAT (SWAT) were dissected and immediately frozen in liquid nitrogen. The plasma and WATs were stored at -80 °C until use. All procedures were approved by the

147 Institutional Animal Care and Use Committee of the Wake Forest University and North
148 Carolina Agricultural and Technical State University.

149 *2.5. Culture and differentiation of 3T3-L1 cells*

150 The 3T3-L1 cells were purchased from the American Type Culture Collection
151 (ATCC®CL173™, Manassas, VA, USA). The cells were maintained in Dulbecco's Modified
152 Eagle's Medium (DMEM) supplemented with 10% calf bovine serum (37 °C, 5% CO_2). To
153 differentiate preadipocytes into white adipocytes, cells were seeded into 12-well plates (BD
154 Biosciences, San Jose, CA, USA) at a density of 1.75 x 10^4 cells/cm^2. When the cells reached
155 confluence (on day 3 after seeding), the medium was changed to DMEM supplemented with
156 10% fetal bovine serum (FBS), 1 μg/mL insulin, 0.5 mM 3-isobutyl-1-methylxanthine and
157 0.25 mM dexamethasone. After two days, the differentiation medium was replaced with post-
158 differentiation medium containing 10% FBS and 1 μg/mL insulin. The cells were cultured for
159 6 days with fresh post-differentiation medium replacements every other day until
160 preadipocytes became fully differentiated into mature white adipocytes (typically by day 11
161 after cell seeding). For experiments, OPE, OPEF and OPWF (50, 100 and 150 μg/mL) and
162 quercetin or isoquercetin (25, 50, and 100 μM) were added to the post-differentiation medium
163 every other day until the cells were harvested for RNA extraction or stained with Oil Red O
164 (day 11).

165 *2.6. Cytotoxicity assay*

166 The cytotoxicities of OPE, OPEF, OPWF, quercetin and isoquercetin were
167 determined using the 3-(4,5-Dimethylthiazol-2-yl)-2,5-Diphenyltetrazolium Bromide (MTT)
168 cell proliferation assay kit (Cayman, Ann Arbor, MI, USA) according to the manufacturer's
169 instructions. Preadipocytes were seeded into 96-well plates at a density of 1.75 x 10^4
170 cells/cm^2. On the following day, OPE, OPEF, and OPWF (0 - 40 μg/mL) and quercetin and

isoquercetin (0 - 240 μM) were added to the cells. After 48 h, the culture medium was replaced with fresh culture medium containing 0.5 mg/mL MTT, and the cells were incubated for 3 h. After removing the MTT-containing medium, 100 μL of dimethyl sulfoxide was added to dissolve the purple formazan crystals. The absorbance that proportionally indicated the number of viable cells was measured at 570 nm using a Synergy HT microplate reader (BioTek, Winooski, VT, USA). Cell viability (%) was calculated as 100 x (absorbance of sample-treated cells / absorbance of the control cells without samples).

2.7. Oil Red O staining

Lipid droplets in the cells were observed by Oil Red O staining (Thermo Fisher Scientific). Fully differentiated white adipocytes (day 11) were washed with phosphate buffered saline (PBS) and rinsed with 10% buffered formalin (Thermo Fisher Scientific). The cells were subsequently incubated with fresh 10% buffered formalin for 1 h at room temperature, washed with 60% isopropanol and completely dried. Cells were further incubated with an Oil Red O working solution, which was prepared by adding 2 parts of water to 3 parts of the stock solution (0.35 g Oil Red O in 100 mL isopropanol) for 30 min at room temperature. After four washes with DW, cells were visualized using an Evos XL-microscope (Thermo Fisher Scientific). To quantitate the lipids in the cells, 1 mL of isopropanol per well was added to dissolve the Oil Red O reagent. The absorbance was measured at 510 nm using a Synergy HT microplate reader (BioTek).

2.8. Quantitative real-time polymerase chain reaction (qPCR) analysis

Total RNA was extracted from the EWATs, RWATs, SWATs and fully differentiated white adipocytes using TRIzol (Thermo Fisher Scientific) according to the manufacturer's instructions. The isolated RNA was quantified using a Take3 micro-volume plate equipped with a Synergy HT microplate reader (BioTek). cDNA was synthesized from

1 μg of total RNA using the XLAScript cDNA MasterMix (Exella GmbH, Feucht, Germany) according to the manufacturer's instructions. Gene expression was quantitated using the Fast Start Essential DNA Green Light Master kit (Roche, Indianapolis, IN, USA) in a Light Cycler 90 (Roche). The PCR conditions were as follows: 10 min at 95 °C, followed by 50 cycles of denaturation for 10 sec at 95 °C, annealing for 10 sec at 60 °C, and extension for 10 sec at 72 °C. The primers were designed using Primer3, a web-based software (http://bioinfo.ut.ee/primer3-0.4.0/), and are listed in Table 1. Ribosomal protein L 32 (RPL32) was used as the invariant gene.

2.9. Inhibition of AMP-activated protein kinase (AMPK)

3T3-L1 cells were treated with dorsomorphin, an AMPK inhibitor, to examine the role of AMPK signaling in the browning of 3T3-L1 cells by quercetin. The cells were cultured and differentiated using the procedure described above. After differentiation, the cell culture medium was replaced with the post-differentiation medium including 5 μM dorsomorphin, 100 μM quercetin, or 5 μM dorsomorphin plus 100 μM quercetin on days 5, 7 and 9. On day 11, the cells were harvested to measure PRDM16, UCP1, PGC1α, and carnitine palmitoyltransferase (CPT) 1α gene expression.

2.10. Statistical analysis

The data are expressed as the mean ± standard error of the mean (SEM). The differences between the control and the various concentrations of OPE, OPEF, OPWF, quercetin, and isoquercetin were evaluated by one-way analysis of variance (ANOVA) with Tukey's post hoc test (Prism 5.0, GraphPad Software Inc., La Jolla, CA, USA). The data obtained from the *in vivo* study and AMPK inhibition experiments were analyzed using the unpaired Student's *t*-test (Prism 5.0, GraphPad Software Inc.). P values less than 0.05 were considered significant.

3. Results

3.1. OPE induces adipocyte browning in WAT

To investigate whether OPE can change the characteristics of white adipocytes to those of brown-like adipocytes in WAT, WAT from HFD-OPE-fed mice were evaluated by comparing them to those of HFD-fed mice. At the end of the 8-week feeding period, the HFD-OPE-fed mice had similar body weights (HFD, 35.0 ± 1.1 g, n = 9; HF-OPE, 35.1 ± 2.2 g, n = 6), EWAT weights (HFD, 2.2 ± 0.2 g, n = 9; HFD-OPE, 2.4 ± 0.3 g, n = 6) and RWAT weights (HFD, 0.70 ± 0.04, n = 9; HF-OPE, 0.74 ± 0.06, n = 6) to those of the HFD-fed mice. Figure 1A-H shows the expression changes of an adipogenesis-related gene (peroxisome proliferator-activated receptor gamma, PPARγ), lipogenesis-related genes (fatty acid synthase, FAS and acetyl-CoA carboxylase, ACC), BAT-specific genes (PRDM16, UCP1, PGC1α, and CIDEA) and a fatty acid oxidation-associated gene (CPT1α) in EWAT, RWAT, and SWAT of HFD-OPE fed mice. OPE did not affect PPARγ expression in the WATs (Fig. A). FAS expression was unchanged in all three WAT types when HFD-OPE-fed mice were compared to HFD-fed mice, whereas ACC was downregulated by nearly 50% in the EWATs but not in the RWATs and SWATs (Fig. 1B and C). Consistent with the expression increase of PRDM16, which encodes a coregulator for brown adipocyte development, the UCP1, PGC1α and CIDEA genes were upregulated in the RWATs of the HFD-OPE-fed mice (Fig. 1D-G). In the SWATs, only UCP1 and CIDEA were upregulated, while the PRDM16 and PGC1α genes remained unchanged (Fig. 1D-G). There was no change in CPT1α gene expression (Fig. 1H).

3.2. OPE induces white adipocytes to become brown like-adipocytes

OPE and OPEF did not exhibit cytotoxicities at or below 150 μg/mL, and OPWF was not cytotoxic at or below 400 μg/mL. Quercetin and isoquercetin did not exhibit cytotoxicities at or below 100 μM and 400 μM, respectively. Thus, the concentration ranges chosen for this 3T3-L1 cell study were 50 to 150 μg/mL for OPE, OPEF and OPWF and 25 μM to 100 μM for quercetin and isoquercetin. Figure 2 shows the browning effect of OPE on adipocytes using 3T3-L1 cells. PPARγ gene expression gradually increased as the treatment concentration increased to 100 μg/mL OPE compared to adipocytes without the OPE treatment, which were used as the control. However, adipocytes treated with 150 μg/mL OPE exhibited an equal expression level to that observed in adipocytes treated with 50 μg/mL OPE (Fig. 2A). As shown in Figure 2B and C, the FAS and ACC genes were unaltered by the 50 and 100 μg/mL OPE treatments, but both genes were decreased by 150 μg/mL OPE. Adipocytes that were treated with 50 and 100 μg/mL OPE showed increased PRDM16 expression levels, but this gene was suppressed by 150 μg/mL OPE (Fig. 2D). However, UCP1 expression was induced by increasing the OPE concentration (Fig. 2E). Treatments with either 100 or 150 μg/mL OPE increased PGC1α expression (Fig. 2F). The CIDEA gene was significantly downregulated by OPE in a dose-dependent manner (Fig. 2G). Consistent with the increased expression of BAT-selective genes, the 100 or 150 μg/mL OPE treatments increased CPT1α expression (Fig. 2H). Adipocyte images that were obtained by Oil Red O staining to visualize lipid droplets are shown in Figure 2I. Adipocytes without OPE treatment showed a single large lipid droplet, which was characteristic of white adipocytes. By increasing the OPE concentration, the lipid droplet contracted and became multiple droplets, and the overall lipid accumulation in the adipocytes was reduced (Fig. 2I and J).

3.3. OPEF, but not OPWF, induces adipocyte browning

We investigated whether OPEF and OPWF, which were fractionated from OPE, exhibited the same browning effect in 3T3-L1 adipocytes. The expression levels of the PPARγ, FAS and ACC genes were decreased by 150 μg/mL OPEF compared with those of the control, but these genes were unchanged in the OPWF-treated adipocytes, as shown in Figure 3A-C. PRDM16 expression was increased in adipocytes treated with 50 and 100 μg/mL OPEF (Fig. 3D). However, its expression was dramatically suppressed by 150 μg/mL OPEF. Adipocytes that were treated with all three OPWF concentrations showed identical inductions in their expression levels of PRDM16 compared with that of the control (Fig. 3D). As shown in Figures 3E and 3F, the UCP1 and PGC1α genes were upregulated in a dose-dependent manner by OPEF. These genes were also moderately induced by OPWF. CIDEA expression was reduced by OPEF, but there was no change in the OPWF-treated adipocytes (Fig. 3G). Consistent with the increased expression of BAT-specific genes, CPT1α was also increased by OPEF but remained unchanged by OPWF (Fig. 3H).

3.4. Quercetin and isoquercetin are the major flavonoids in OPE, OPEF, and OPWF

To identify and quantify the major dietary compounds in OPE, OPEF, and OPWF, three extracts were analyzed by HPLC. The chromatograms of the quercetin and isoquercetin separations from OPE, OPEF, and OPWF by HPLC are shown in Figure 4A-C. According to the standard curve-based quantification of pure quercetin and isoquercetin, the quercetin and isoquercetin concentrations in OPE and OPEF were 6.8 ± 0.1 mg and 8.1 ± 0.1 mg/100 mg dried weight (dw) and 7.8 ±0.1 mg and 9.1 ± 0.1 mg/100 mg dw, respectively. Further calculations showed that the OPE and OPEF used in our cell study contained mixtures of up to 12.15 μg/mL isoquercetin (26.16 μM) plus 10.2 μg/mL (33 μM) quercetin and 13.65 μg/mL isoquercetin (29.4 μM) plus 11.69 μg/mL (38.7 μM) quercetin, respectively. As

shown in Figure 4C, an isoquercetin peak was observed in OPWF with a lower limit of quantification. Quercetin was not detected in OPWF (Fig. 4C).

3.5. Quercetin, but not isoquercetin, changes the characteristics of adipocytes to those of BAT-like adipocytes

We investigated the effects of the major dietary compounds found in OPE and OPEF, quercetin and isoquercetin, on adipocyte browning. The 100 μM quercetin treatment slightly increased PPARγ gene expression but decreased FAS and ACC gene expression (Fig. 5A-C). PRDM16 was upregulated in adipocytes that were treated with either 50 or 100 μM quercetin. However, adipocytes that were treated with 100 μM quercetin showed the same PRDM16 expression level as the control (Fig. 5D). When treated with 100 μM quercetin, expression of the UCP1 and PGC1α genes was significantly increased (Fig. 5E and F). CIDEA was reduced by increasing the concentration of quercetin (Fig. 5D). Consistent with the increased expression of BAT-specific genes, CPT1α was also increased by quercetin (Fig. 5H). None of the genes tested in this study were affected by isoquercetin (Fig. 5A-H).

3.6. Quercetin partially regulates adipocyte browning through the AMPK signaling pathway

To determine the mechanism by which quercetin converts the characteristics of white adipocytes to those of BAT-like adipocytes, the expression of BAT-specific genes was examined using 3T3-L1 adipocytes treated with or without 100 μM quercetin in the absence or presence of an AMPK inhibitor (dorsomorphin). As shown in Figure 6A, dorsomorphin decreased PRDM16 gene expression to the level observed in adipocytes treated with quercetin in the absence of dorsomorphin. There was no additional reduction by quercetin (Fig. 6A). Dorsomorphin increased UCP1 gene expression (Fig. 6B), and the induction was increased further with quercetin. PGC1α gene expression was increased by quercetin (Fig.

316 6C), but this effect was not observed in the AMPK-inhibited adipocytes (Fig. 6C). CPT1α
317 was upregulated in quercetin-treated adipocytes, but this effect was not observed with AMPK
318 inhibition (Fig. 6D).
319
320 **4. Discussion**
321 This study used HFD-induced obese mice and 3T3-L1 cells to examine whether
322 onion peel exhibits a browning effect, where white adipocytes are converted to brown-like
323 adipocytes. Several studies have provided evidence that onion peel has the potential to
324 alleviate obesity by inhibiting adipogenesis and increasing fatty acid oxidation. However, the
325 onion peel-mediated browning effect that may prevent obesity has not been investigated. In
326 this study, OPE supplementation for 8 weeks did not lower body weight or fat mass in HFD-
327 induced obesity, but the HFD-OPE groups showed increased expression of several BAT-
328 specific genes (PRDM16, UCP1, PGC1α and CIDEA) in their RWATs and SWATs.
329 PRDM16, a transcriptional coregulator, is essential for brown adipocyte development
330 in BAT and beige cells in WAT [8]. Together with the increased PRDM16 expression in this
331 study, UCP1, a BAT-specific thermogenin, and PGC1α, a transcriptional factor that regulates
332 UCP1-induced thermogenesis, were induced in both the RWATs and SWATs of HFD-OPE-
333 fed mice. PGC1α positively regulates CIDEA expression by stimulating estrogen-related
334 receptor (ERR) α and nuclear respiratory factor (NRF)-1 [19]. CIDEA, another BAT-specific
335 gene, plays a major role in lipid droplet formation in BAT and beige cells [19, 20]. Consistent
336 with the increased PGC1α expression, CIDEA was dramatically induced in the RWATs of
337 HFD-OPE-fed mice. Beige cells develop in response to stimuli (i.e., exposure to cold
338 temperatures) in SWAT, which is an abundantly inguinal fat, and in RWAT [21] [22]. In this
339 study, the HFD-OPE-fed mice showed an increase in all BAT-specific genes in their
340 RWATs, but only the UCP1 and CIDEA genes were induced in their SWATs. None of the

341 BAT-specific genes were increased in the EWATs by OPE supplementation. Although OPE
342 did not reduce WAT weights during 8-week feeding, long-term OPE consumption may
343 prevent fat accumulation by changing the characteristics of adipocytes to those of brown-like
344 adipocytes in WAT.

345 To investigate functional compounds for the browning effects of OPE, we added
346 OPE, OPEF, OPWF, quercetin, and isoquercetin to 3T3-L1 cells during their post-
347 differentiation phase. Consistent with the increased expression of BAT-specific genes in the
348 RWATs of the HFD-OPE-fed mice, OPE induced PRDM16, UCP1 and PGC1α, but not
349 CIDEA expression, in mature white adipocytes. Recently, CIDEA has been reported to
350 promote lipid droplet enlargement by transferring triacylglycerol between lipid droplets [23].
351 CIDEA-deficient mice, which are resistant to obesity development, showed increased non-
352 shivering thermogenesis in BAT after being exposed to cold temperatures [24]. In this study,
353 OPE-treated 3T3-L1 cells exhibited reduced expression of the CIDEA gene. This reduction is
354 typically associated with a decline in fat accumulation and with small lipid droplets. BAT-
355 specific genes were associated with the regulation of lipolysis and lipogenesis. Together with
356 the increase in UCP1 expression, CPT1α was upregulated in the OPE-treated 3T3-L1 cells.
357 This result suggests that OPE may induce lipolysis for fatty acid oxidation, further activating
358 UCP1 expression. In contrast to the *in vivo* study, OPE increased PPARγ at lower
359 concentrations but reduced PPARγ, FAS, and ACC expression at 150 μg/mL in the 3T3-L1
360 cells, which suggests decreased adipogenesis and lipogenesis. The inhibition of adipogenesis
361 by OPE may have also resulted from ACC inactivation through AMPK activation by
362 quercetin, a bioactive compound of the onion peel [16]. OPE-mediated inhibition of
363 adipogenesis and lipogenesis in 3T3-L1 cells has been previously reported [15, 17].

364 OPE was fractionated into its hydrophobic and hydrophilic fractions (OPEF and
365 OPWF, respectively). In this study, OPEF-treated 3T3-L1 cells showed similar browning

366 effects to those observed in OPE-treated adipocytes. OPWF did not affect the genes involved
367 in regulating adipogenesis, lipogenesis, and fatty acid oxidation or the BAT-specific genes.
368 This result indicates that OPEF contained functional compounds that could convert white
369 adipocytes to brown-like adipocytes. A previous study showed that isoquercetin and
370 quercetin are major compounds in the onion and onion peel [25]. Our data, obtained by
371 HPLC, revealed the presence of these two compounds in OPE and OPEF. Our data suggested
372 that OPE and OPEF, which we used in the cell study, comprised similar concentrations of
373 isoquercetin and quercetin. However, only quercetin induced the gene expression pattern
374 observed in the OPE- and OPEF-treated adipocytes. This finding indicates that quercetin is a
375 functional compound in onion peel that converts the characteristics of white adipocytes to
376 those of brown-like adipocytes.

377 Several reports have shown that white adipocyte browning is mediated by the AMPK
378 signaling cascade [10, 14, 26, 27]. AMPK is a key regulator of energy balance that stimulates
379 catabolic ATP-generating pathways (i.e., fatty acid oxidation), induces mitochondrial
380 biogenesis and activates BAT [28, 29]. Wang et al. showed that resveratrol increased BAT-
381 specific gene expression in the inguinal WATs of mice by activating the phosphorylation of
382 AMPK α1 [14]. The browning effect of curcumin in 3T3-L1 cells was also achieved by
383 inducing AMPK [10]. Additionally, quercetin is a known activator of the AMPK cascade
384 [16]. Therefore, we investigated whether the observed quercetin-induced browning effect was
385 mediated by AMPK activation. When AMPK was inhibited, the basal mRNA levels of
386 PRDM16, PGC1α and CPT1α were reduced, and this decline was not reversible with
387 quercetin. However, the dorsomorphin-treated cells showed an increase in UCP1 gene
388 expression compared with that of cells without dorsomorphin. Quercetin still increased UCP1
389 gene expression when AMPK was inhibited, indicating that the quercetin-induced browning

effect was, in part, AMPK-dependent. However, there may be alternative mechanisms by which quercetin promotes adipocyte browning to brown-like adipocytes.

Overall, OPE promoted the remodeling of white adipocytes to brown-like adipocytes by inducing BAT-like genes in the WATs of mice and in 3T3-L1 cells *in vitro*. The OPE-induced browning effect was mediated by quercetin, a functional compound in onion peel whose effect was partially dependent on the AMPK signaling cascade. Although further animal studies are necessary to investigate the long-term effects of exposure to OPE or quercetin and to uncover the mechanisms behind quercetin's regulation of the browning effect, our findings are the first to report the browning effects of onion peel and quercetin *in vivo* and *in vitro*. This study demonstrates the anti-obesity effect of onion peel through adipocyte browning in WAT. The onion peel, a by-product that contains a high concentration of quercetin, may be a potential candidate for development into food products that economically prevent obesity.

Acknowledgements

The onion peels were kindly provided by Boardman Foods Inc. (Boardman, Oregon, USA).

Figure Legends

Figure 1. The OPE effect on gene expression in WATs. Expression changes were measured in the EWATs, RWATs and SWATs of mice that were fed HFD (n = 9) and HFD-OPE (n = 6) for 8 weeks. Expression of selected genes related to adipogenesis, (A) PPARγ, and lipogenesis, (B) FAS and (C) ACC. Other genes included the BAT-specific genes—(D) PRDM16, (E) UCP1, (F) PGC1α, and (G) CIDEA—and one fatty acid oxidation-associated gene, (H) CPT1α. *$P < 0.05$, HFD vs. HFD-OPE.

Figure 2. The OPE effect on gene expression in 3T3-L1 adipocytes. Gene expression was determined in 3T3-L1 adipocytes that were treated with or without OPE (0, 50, 100 and 150 μg/mL) every other day during differentiation (days 5, 7, and 9). The selected genes related to adipogenesis, (A) PPARγ, and lipogenesis, (B) FAS and (C) ACC. Other genes included the BAT-specific genes—(D) PRDM16, (E) UCP1, (F) PGC1α, and (G) CIDEA—and one fatty acid oxidation-associated gene, (H) CPT1α. (I) Lipid droplets were visualized after Oil Red O staining in fully differentiated 3T3-L1 adipocytes that were treated with OPE (0, 50, 100 and 150 μg/mL). (J) Lipid accumulation in fully differentiated 3T3-L1 adipocytes was quantified after extracting the Oil Red O stain. A different letter indicates a statistically significant difference ($P < 0.05$).

Figure 3. The effect of OPEF and OPWF on gene expression in 3T3-L1 adipocytes. Gene expression was determined in 3T3-L1 adipocytes that were treated with or without OPEF and OPWF (0, 50, 100 and 150 μg/mL) every other day during differentiation (days 5, 7, and 9). The selected genes related to adipogenesis, (A) PPARγ, and lipogenesis, (B) FAS and (C) ACC. Other genes included the BAT-specific genes—(D) PRDM16, (E) UCP1, (F) PGC1α,

and (G) CIDEA—and one fatty acid oxidation-associated gene, (H) CPT1α. A different letter indicates a statistically significant difference ($P < 0.05$).

Figure 4. Identification of isoquercetin and quercetin in OPE, OPEF and OPWF. Isoquercetin and quercetin were detected in OPE, OPEF and OPWF by HPLC.

Figure 5. The effect of OPEF and OPWF on gene expression in 3T3-L1 adipocytes. Gene expression was determined in 3T3-L1 adipocytes that were treated with or without quercetin and isoquercetin (0, 25, 50 and 100 μM) every other day during differentiation (days 5, 7, and 9). The selected genes related to adipogenesis, (A) PPARγ, and lipogenesis, (B) FAS and (C) ACC. Other genes included the BAT-specific genes—(D) PRDM16, (E) UCP1, (F) PGC1α, and (G) CIDEA—and one fatty acid oxidation-associated gene, (H) CPT1α. A different letter indicates a statistically significant difference ($P < 0.05$). QCT, quercetin; IsoQCT, isoquercetin

Figure 6. The effect of quercetin on the expression of BAT-specific genes under AMPK inhibition. Gene expression of (A) PRDM16, (B) UCP1, (C) PGC1α, and (D) CPT1α was determined in 3T3-L1 adipocytes that were treated with or without 100 μM quercetin (on days 5, 7, and 9) in the absence or presence of an AMPK inhibitor (5 μM dorsomorphin). *$P < 0.05$, without quercetin vs. with quercetin; **$P < 0.01$, without quercetin vs. with quercetin.

464

465 **References**

466 [1] Hill JO, Wyatt HR, Peters JC. Energy balance and obesity. Circulation. 2012;126:126-32.

467 [2] Bjorntorp P. Obesity: a chronic disease with alarming prevalence and consequences. J

468 Intern Med. 1998;244:267-9.

469 [3] Cypess AM, Lehman S, Williams G, Tal I, Rodman D, Goldfine AB, et al. Identification

470 and importance of brown adipose tissue in adult humans. N Engl J Med. 2009;360:1509-17.

471 [4] Gilsanz V, Hu HH, Kajimura S. Relevance of brown adipose tissue in infancy and

472 adolescence. Pediatr Res. 2013;73:3-9.

473 [5] Fruhbeck G, Becerril S, Sainz N, Garrastachu P, Garcia-Velloso MJ. BAT: a new target

474 for human obesity? Trends Pharmacol Sci. 2009;30:387-96.

475 [6] Kozak LP, Anunciado-Koza R. UCP1: its involvement and utility in obesity. Int J Obes.

476 2008;32 Suppl 7:S32-8.

477 [7] Yang WL, Perillo W, Liou D, Marambaud P, Wang P. AMPK inhibitor compound C

478 suppresses cell proliferation by induction of apoptosis and autophagy in human colorectal

479 cancer cells. J Surg Oncol. 2012;106:680-8.

480 [8] Kajimura S. Promoting brown and beige adipocyte biogenesis through the PRDM16

481 pathway. Int J Obes Suppl. 2015;5:S11-4.

482 [9] Cao L, Choi EY, Liu X, Martin A, Wang C, Xu X, et al. White to brown fat phenotypic

483 switch induced by genetic and environmental activation of a hypothalamic-adipocyte axis.

484 Cell Metab. 2011;14:324-38.

485 [10] Lone J, Choi JH, Kim SW, Yun JW. Curcumin induces brown fat-like phenotype in

486 3T3-L1 and primary white adipocytes. J Nutr Biochem. 2016;27:193-202.

487 [11] Zhang Z, Zhang H, Li B, Meng X, Wang J, Zhang Y, et al. Berberine activates

488 thermogenesis in white and brown adipose tissue. Nat Commun. 2014;5:5493.

[12] Baboota RK, Singh DP, Sarma SM, Kaur J, Sandhir R, Boparai RK, et al. Capsaicin induces "brite" phenotype in differentiating 3T3-L1 preadipocytes. PLoS One. 2014;9:e103093.

[13] Lone J, Yun JW. Monoterpene limonene induces brown fat-like phenotype in 3T3-L1 white adipocytes. Life Sci. 2016;153:198-206.

[14] Wang S, Liang X, Yang Q, Fu X, Rogers CJ, Zhu M, et al. Resveratrol induces brown-like adipocyte formation in white fat through activation of AMP-activated protein kinase (AMPK) alpha1. Int J Obes. 2015;39:967-76.

[15] Moon J, Do HJ, Kim OY, Shin MJ. Antiobesity effects of quercetin-rich onion peel extract on the differentiation of 3T3-L1 preadipocytes and the adipogenesis in high fat-fed rats. Food Chem Toxicol. 2013;58:347-54.

[16] Ahn J, Lee H, Kim S, Park J, Ha T. The anti-obesity effect of quercetin is mediated by the AMPK and MAPK signaling pathways. Biochem Biophys Res Commun. 2008;373:545-9.

[17] Bae CR, Park YK, Cha YS. Quercetin-rich onion peel extract suppresses adipogenesis by down-regulating adipogenic transcription factors and gene expression in 3T3-L1 adipocytes. J Sci Food Agric. 2014;94:2655-60.

[18] Kim KA, Yim JE. Antioxidative activity of onion peel extract in obese women: a randomized, double-blind, placebo controlled study. J Cancer Prev. 2015;20:202-7.

[19] Hallberg M, Morganstein DL, Kiskinis E, Shah K, Kralli A, Dilworth SM, et al. A Functional Interaction between RIP140 and PGC-1α Regulates the Expression of the Lipid Droplet Protein CIDE. Mol Cell Biol. 2008;28:6785–95.

[20] Wu L, Zhou L, Chen C, Gong J, Xu L, Ye J, et al. Cidea controls lipid droplet fusion and lipid storage in brown and white adipose tissue. Sci China Life Sci. 2014;57:107-16.

513 [21] Hsieh CH, Chen GC, Chen PH, Wu TF, Chao PM. Altered white adipose tissue protein
514 profile in C57BL/6J mice displaying delipidative, inflammatory, and browning characteristics
515 after bitter melon seed oil treatment. PLoS One. 2013;8:e72917.
516 [22] Betz MJ, Slawik M, Lidell ME, Osswald A, Heglind M, Nilsson D, et al. Presence of
517 brown adipocytes in retroperitoneal fat from patients with benign adrenal tumors: relationship
518 with outdoor temperature. J Clin Endocrinol Metab. 2013;98:4097-104.
519 [23] Barneda D, Planas-Iglesias J, Gaspar ML, Mohammadyani D, Prasannan S, Dormann D,
520 et al. The brown adipocyte protein CIDEA promotes lipid droplet fusion via a phosphatidic
521 acid-binding amphipathic helix. Elife. 2015;4:e07485.
522 [24] Zhou Z, Yon Toh S, Chen Z, Guo K, Ng CP, Ponniah S, et al. Cidea-deficient mice have
523 lean phenotype and are resistant to obesity. Nat Genet. 2003;35:49-56.
524 [25] Ko EY, Nile SH, Sharma K, Li GH, Park SW. Effect of different exposed lights on
525 quercetin and quercetin glucoside content in onion (Allium cepa L.). Saudi J Biol Sci.
526 2015;22:398-403.
527 [26] Mulligan JD, Gonzalez AA, Stewart AM, Carey HV, Saupe KW. Upregulation of
528 AMPK during cold exposure occurs via distinct mechanisms in brown and white adipose
529 tissue of the mouse. J Physiol. 2007;580:677-84.
530 [27] Ahmadian M, Abbott MJ, Tang T, Hudak CS, Kim Y, Bruss M, et al. Desnutrin/ATGL
531 is regulated by AMPK and is required for a brown adipose phenotype. Cell Metab.
532 2011;13:739-48.
533 [28] Viollet B, Horman S, Leclerc J, Lantier L, Foretz M, Billaud M, et al. AMPK inhibition
534 in health and disease. Crit Rev Biochem Mol Biol. 2010;45:276-95.
535 [29] Bijland S, Mancini SJ, Salt IP. Role of AMP-activated protein kinase in adipose tissue
536 metabolism and inflammation. Clinical science. 2013;124:491-507.
537

Gene	**Forward primer**	**Reverse primer**
ACC	TGCATTCTGACCTTCACGAC	ACATCCACTTCCACACACGA
CIDEA	ATCACAACTGGCCTGGTTACG	TACTACCCGGTGTCCATTTCT
CPT1α	TTTGACTTTGAGAAATACCCTGATA	TGGATGAAATTCTCTCCCACAATAA
FAS	TGGGTTCTAGCCAGCAGAGT	ACCACCAGAGACCGTTATGC
PGC1α	TGCCCAGATCTTCCTGAACT	TCTGTGAGAACCGCTAGCAA
PPARγ	TTTGACTTTGAGAAATACCC	TGGATGAAATTCTCTCCAC
PRDM16	CAGCACGGTGAAGCCATTC	GCGTGCATCCGCTTGTG
RPL32	CACCAGTCAGACCGATAT	TTCTCCGCACCCTGTTG
UCP1	TCAGGATTGGCCTCTACGAC	TGCATTCTGACCTTCACGAC

538 Table 1. Quantitative real-time PCR primers

539

540 Abbreviations: ACC, acetyl-CoA carboxylase; CIDEA, cell death-inducing DFFA-like
541 effector; CPT1α, carnitine palmitoyltransferase 1 alpha; FAS, fatty acid synthase; PGC1α,
542 peroxisome proliferator-activated receptor gamma coactivator 1 alpha; PPARγ, peroxisome
543 proliferator-activated receptor gamma; PRDM16, PR domain-containing 16; RPL32,
544 ribosomal protein L 32; UCP1, uncoupling protein 1

545

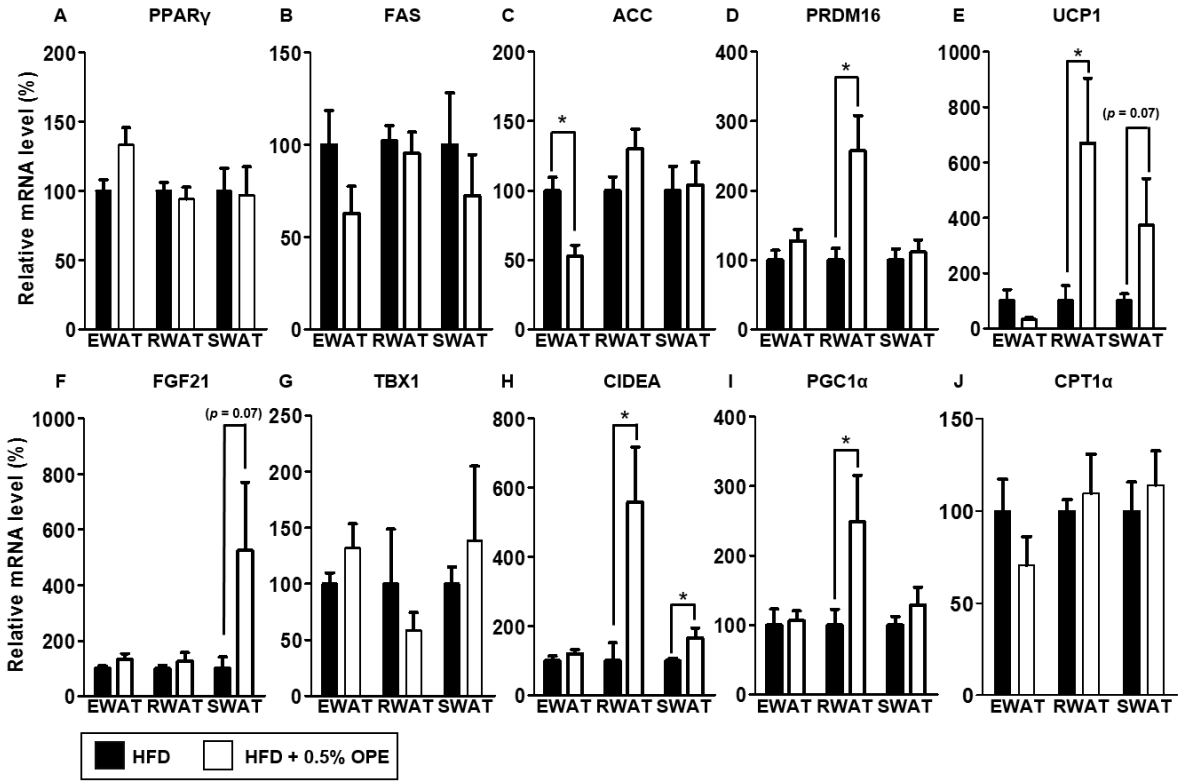

Figure 1

546

547

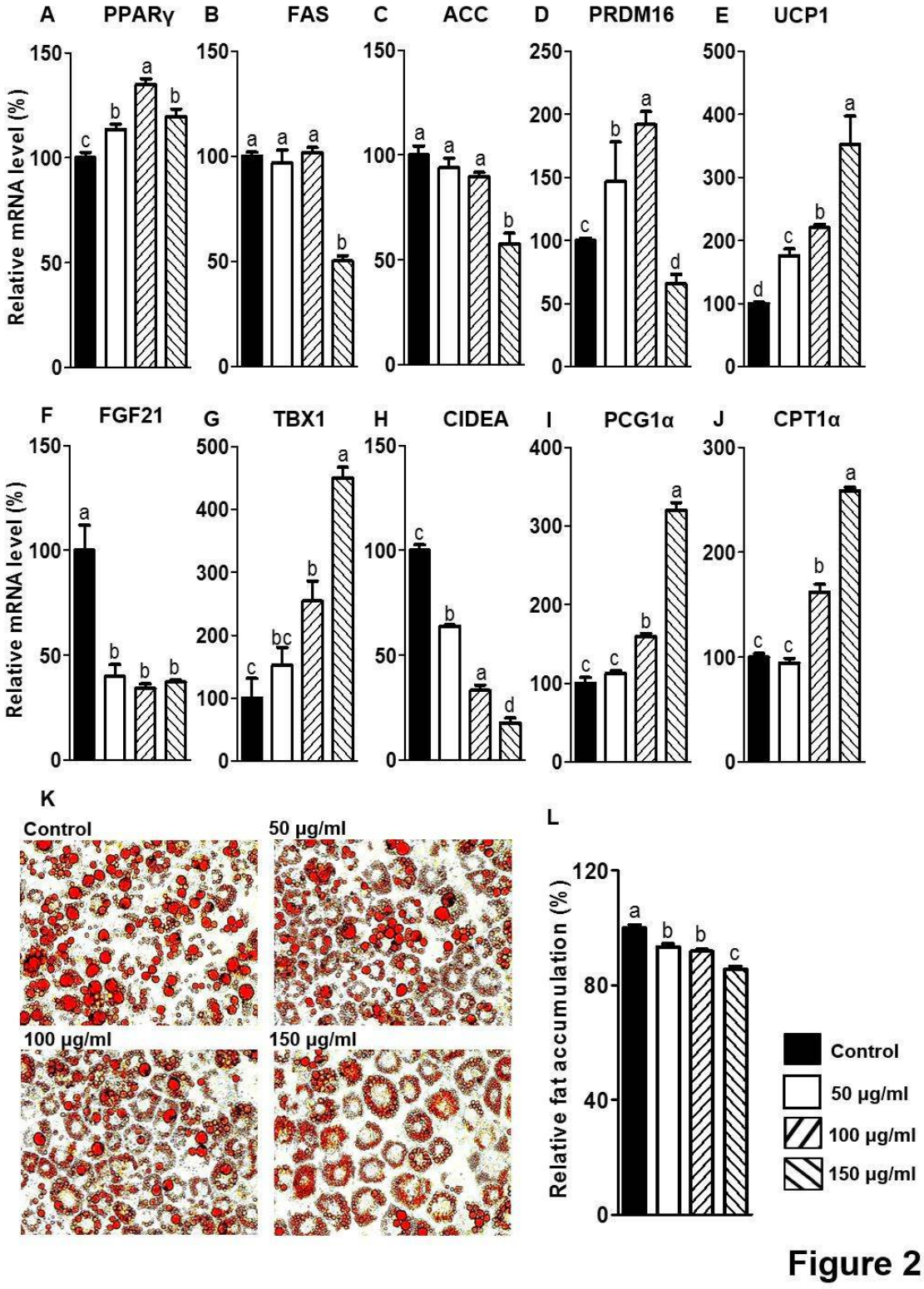
A PPARγ
B FAS
C ACC
D PRDM16
E UCP1
F FGF21
G TBX1
H CIDEA
I PCG1α
J CPT1α
Relative mRNA level (%)
K
Control
50 μg/ml
100 μg/ml
150 μg/ml
L
Relative fat accumulation (%)
Control
50 μg/ml
100 μg/ml
150 μg/ml

Figure 2

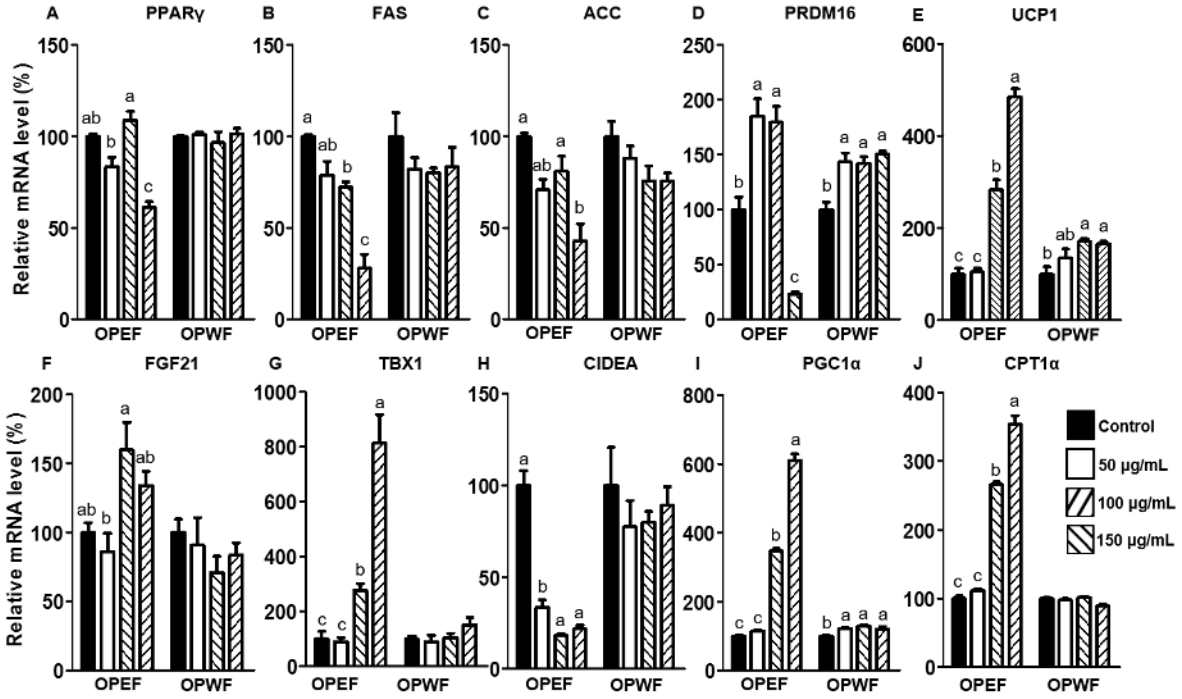
A
PPARγ
B
FAS
C
ACC
D
PRDM16
E
UCP1
F
FGF21
G
TBX1
H
CIDEA
I
PGC1α
J
CPT1α
Relative mRNA level (%)
OPEF
OPWF
Control
50 μg/mL
100 μg/mL
150 μg/mL

Figure 3

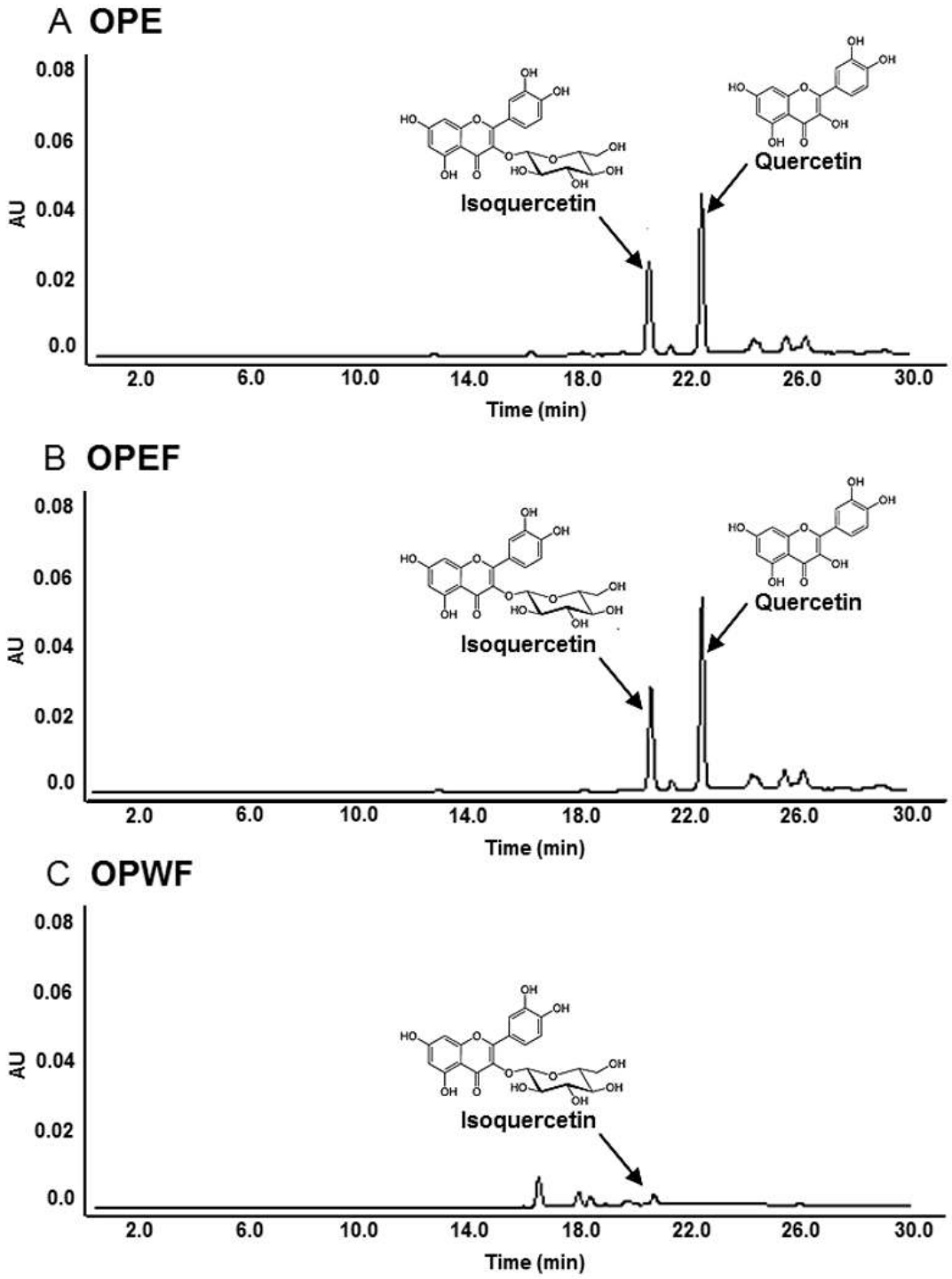

Figure 4

552

553

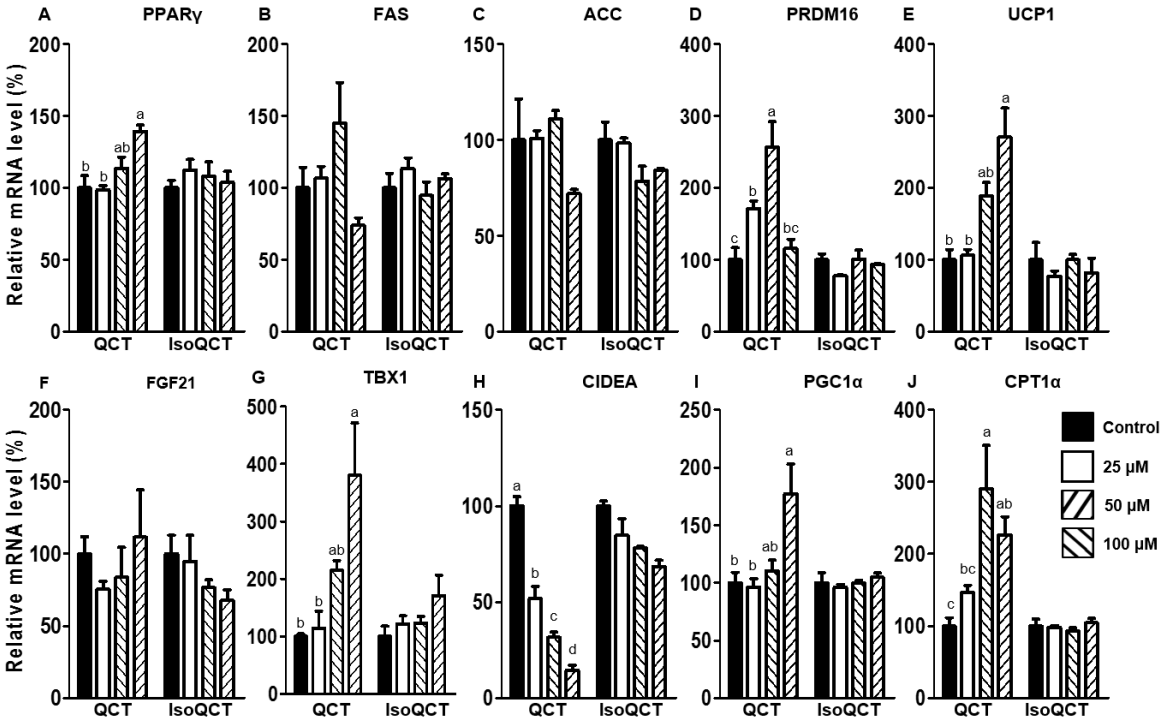

Figure 5

554

555

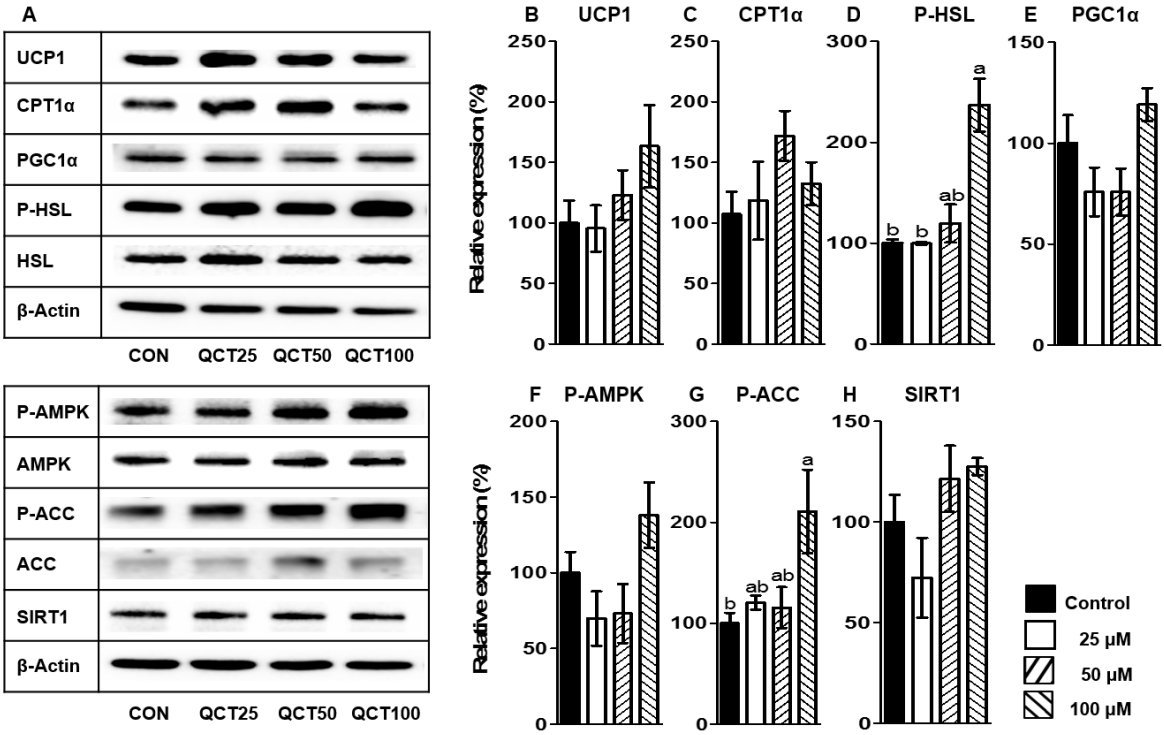

Figure 6

556

557

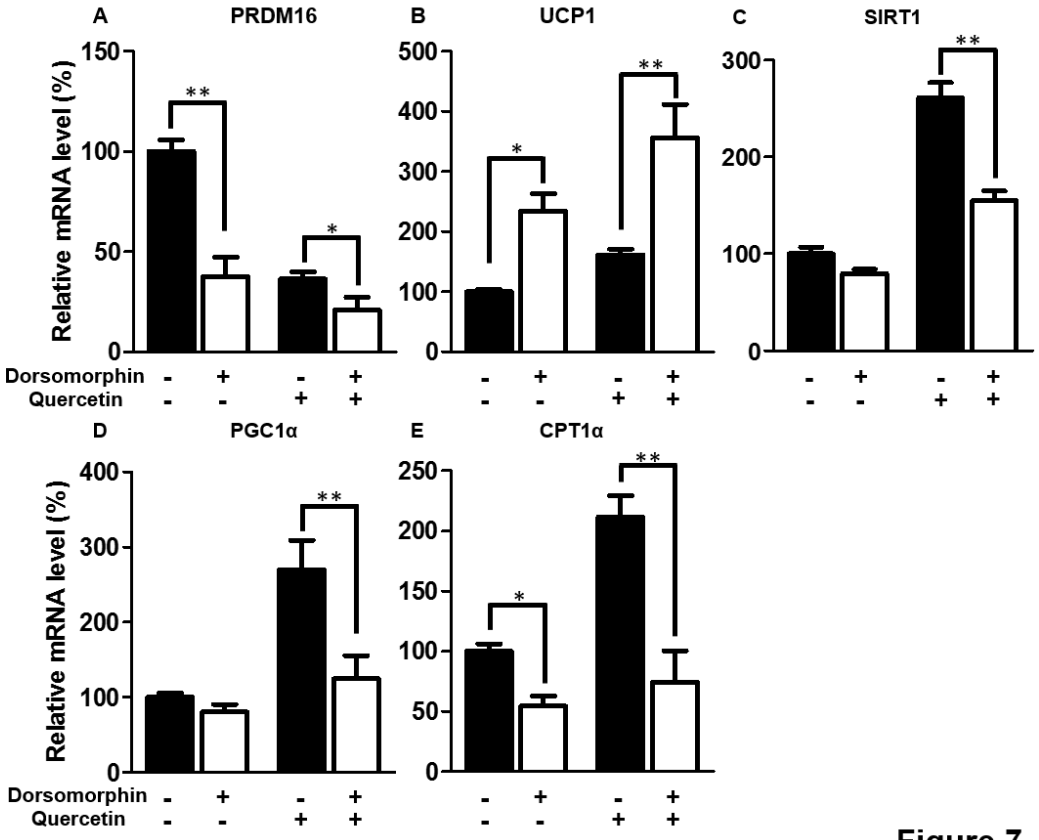
A
PRDM16
B
UCP1
C
SIRT1
D
PGC1α
E
CPT1α
Relative mRNA level (%)
Dorsomorphin
Quercetin

Figure 7

558